



Durable dual-methylpiperidinium crosslinked poly(binaphthyl-co-terphenyl piperidinium) anion exchange membranes with high ion transport and electrochemical performance

Wei Ting Gao ^{a,1}, Xue Lang Gao ^{a,1}, Yvonne Shuen Lann Choo ^b, Jia Jun Wang ^a, Zhi Hong Cai ^a, Qiu Gen Zhang ^a, Ai Mei Zhu ^a, Qing Lin Liu ^{a,*}

^a Department of Chemical & Biochemical Engineering, Fujian Provincial Key Laboratory of Theoretical and Computational Chemistry, The College of Chemistry and Chemical Engineering, Xiamen University, Xiamen 361005, P. R. China

^b School of Energy and Chemical Engineering, Xiamen University Malaysia, Sepang 43900, Selangor Darul Ehsan, Malaysia

ARTICLE INFO

Keywords:

Dual-piperidinium crosslinking
Ion transport
Alkaline stability
Fuel cells
Water electrolysis

ABSTRACT

A series of novel crosslinked poly(binaphthyl-co-terphenyl piperidinium)s (QBNTPs) based on various dual-piperidinium crosslinkers are designed and prepared as anion exchange membranes (AEMs) for alkaline fuel cells and water electrolysis. The excellent alkaline stability of the dual-piperidinium crosslinker with methyl substituent on the C4-position of the piperidinium ring is first confirmed. The as-prepared dual-methylpiperidinium crosslinked poly(binaphthyl-co-terphenyl piperidinium) (QBNTP-MP11) AEM shows an exceptional OH⁻ conductivity (181.2 mS cm⁻¹) and a suppressed swelling ratio (19.7%) at 90 °C. QBNTP-MP11 also exhibits a superior toughness (6.08 MJ m⁻³) and a marked storage modulus (6.52 × 10⁶ Pa). Additionally, having less than 5% OH⁻ conductivity deterioration after being treated in 2 M NaOH at 80 °C for 1560 h, QBNTP-MP11 demonstrates an outstanding durability. Notably, QBNTP-MP11 can achieve a high peak powder density of 1.41 W cm⁻² in a single cell test and an excellent current density of 2.7 A cm⁻² at 2.0 V in alkaline water electrolysis. Meanwhile, QBNTP-MP11 demonstrates a desirable durability in a single cell operation and water electrolysis. All those results validate that the durable and robust QBNTP-MP11 has a good application perspective. The work is anticipated to provide a valuable guidance for the design of new stable and high-performance AEMs.

1. Introduction

The polyelectrolyte membrane-based energy conversion and storage devices have received increasing interest owing to their great potential for addressing non-renewable-energy shortages and global warming. Among them, fuel cells are the prospective device to generate electricity by utilizing clean hydrogen energy in an eco-friendly and efficient electrochemical process [1–3], whereas water electrolysis is the potential device for hydrogen production by splitting water cleanly and sustainably [4–6]. The anion exchange membranes (AEMs), which are a component of anion exchange membrane fuel cells (AEMFCs) or anion exchange membrane water electrolysis (AEMWE), are responsible for the transport of anions and water molecules and have been advanced quickly. However, relative to commercial benchmark Nafion proton exchange membranes (PEMs), most of the existing AEMs exhibit

undesirable alkaline resistance due to chemically unstable cation groups and polymer backbones in high-pH environments, which significantly limit their practical applications [7,8].

Various cationic groups have been extensively explored, including quaternary ammonium (QA) [9], imidazolium [10], pyrrolidinium [11], piperidinium [12], phosphonium [13], and metal–organic cations [14]. Unfortunately, in a caustic alkaline environment, the majority of these cations are vulnerable to the OH⁻ attack and degrade via nucleophilic substitution (S_N2), Hofmann degradation, Ylide, as well as rearrangement reactions [15]. Numerous efforts have been taken into optimizing the cation structures of the AEMs to promote the alkaline stability. Tang et al. synthesized the chemically stable cobaltocenium cations by reasonably installing alkyl groups based on the consideration of electronic and steric effects [16]. Holdcroft et al. prepared a durable C2-substituted benzimidazolium ring to reinforce the alkaline stability of

* Corresponding author.

E-mail address: qlliu@xmu.edu.cn (Q. Lin Liu).

¹ These authors contributed equally.

AEMs [17]. Yan et al. successfully synthesized many imidazolium groups with high alkaline stability via introducing substituents [18,19]. Sun et al. recently designed ultra-stable piperidinium cations on the basis of the electronic and steric effects of α -C substituents [20]. Lee et al. provided a fascinating insight into the influence of γ -substituted groups on the long-term stability of N-heterocyclic ammonium cations [1].

Advanced AEM materials with ether-free polymer frameworks have attracted widespread attention in recent years, as a promising alternative to traditional AEM materials with ether-containing backbones, due to their remarkable chemical durability resulting from the absence of alkaline-sensitive ether linkages [21]. In the boom of ether-free polymers, poly(arylene)-based polymer backbones prepared by an acid-catalyzed polycondensation are popular due to their extraordinary durability and facile synthetic procedures [22–24]. However, these materials still have some shortcomings that limit their large-scale commercialization. Quaternized poly(arylene piperidinium) (QAPAP) AEMs with an excessive ion content, particularly quaternized poly(biphenyl piperidinium) (QAPBP) counterpart, often exhibit serious dimensional swelling, jeopardizing their mechanical properties and durability [25]. Introducing bulky rigid aromatic structures into the polymer backbones can prevent chain stack and increase inner free volume to develop ionic transport ability. However, the bulky aromatic groups tend to increase the membrane rigidity and brittleness, resulting in undesired mechanical properties [26]. Many strategies, including side-chain grafting [27], crosslinking [28] and blending [29], have been used to limit water swelling and reinforce mechanical properties of these AEMs.

Crosslinking provides a helpful pathway that effectively facilitates the development of AEM performance. However, conventional crosslinkers composed of the hydrophobic structures are usually constructed against the ionic conductivity of AEMs [30]. Many researchers have conducted extensive studies on the optimum structure of crosslinkers to improve physicochemical durability and accelerate anion conduction of AEMs [28]. Zhu et al. investigated the effects of the length of the hydrophilic multi-cation crosslinker on membrane performance and discovered that hexyl spacers between polymer main chains and QA groups in the crosslinker could maintain a reasonable balance between high conductivity and moderate dimensional stability [31]. Lee et al. prepared highly conductive, stable, and robust dual-piperidinium crosslinked polyaromatic-based AEMs by tuning the alkyl spacer in a crosslinker [32]. Piperidinium cation group is prominently stable under a harsh alkaline condition owing to the low ring strain and effective steric protection provided by the symmetrical six-membered-ring structure. However, there is a significant variance in the alkaline-resistant capability of piperidinium cations with different substituents. Up to now, there have been few publications on the effect of various crosslinkers containing piperidinium-based cation groups on the membrane properties. Therefore, enriching and optimizing the piperidinium-based crosslinker through molecular structure design for advanced AEM materials is imperative.

In this work, we synthesized three types of dual-piperidinium crosslinkers tethered with flexible hexane spacers and preliminarily investigated the influence of substituents on properties of crosslinkers from experimental and computational analysis. Afterward, three types of dual-piperidinium-crosslinked AEMs based on chemically stable ether-free poly(binaphthyl-co-terphenyl piperidinium) (QBNTP) backbones were successfully synthesized, while a non-crosslinked AEM with the same main chain was served as a control. The bulky binaphthyl units introduced in the polymer backbones can improve the ionic conduction by enlarging free volume inside the AEMs. Additionally, the incorporation of a flexible dual-piperidinium crosslinker in the ether-free QBNTP main chain can enhance the ionic conductivity and chemical stability by establishing distinct microphase separations and constructing adequate ion conductive highways. The relationship between the structure and properties of these AEMs in this work is thoroughly

studied. Furthermore, electrochemical performance of the prepared AEMs in a single cell and water electrolysis is further evaluated. With superb ionic conductivity, robust alkaline stability, and excellent electrochemical performance, the potential application of the as-prepared AEMs is highlighted.

2. Experimental section

2.1. Materials

p-Terphenyl (TP), binaphthyl (BN), trifluoromethanesulfonic acid (TFSA), trifluoroacetic acid (TFA), piperidine hydrochloride (HP), 4-methylpiperidine (MP), 4-phenylpiperidine (PP), 1,6-dibromohexane (DBH) and CH_3I were purchased from J&K Scientific (Beijing). Ethyl acetate (EA), acetonitrile (CH_3CN), anhydrous ether, dichloroethane (DCM), dimethyl sulfoxide (DMSO), anhydrous ethanol (EtOH), methanol (MeOH), NaOH, K_2CO_3 and Na_2SO_4 were supplied by Sinopharm Chemical Reagent (Shanghai). 1-Methyl-4-piperidone, DMSO-d₆, CD_3OD and D₂O were purchased from Aladdin (Shanghai). All chemicals and reagents were analytical grade and used directly.

2.2. Synthesis of materials

2.2.1. Synthesis of crosslinkers and polymers

Three kinds of crosslinkers: dual-piperidinium (QDHP), dual-methylpiperidinium (QDMP) and dual-phenylpiperidinium (QDPP) were synthesized according to a modified procedure in the literature [33] and detailed in the Supporting Information (SI). The synthetic procedure of the poly(binaphthyl-co-terphenyl piperidine) (BNTP) copolymer via a super-acid polymerization reaction was described in the SI.

2.2.2. Quaternization

All of the polyelectrolytes were fabricated by a Menshutkin reaction. Taking the dual-piperidinium crosslinked poly(binaphthyl-co-terphenyl piperidinium) (QBNTP-HP10) polyelectrolyte as an example, BNTP (2.00 g, 6 mmol), K_2CO_3 (0.80 g, 3 mmol), QDHP (0.50 g, 0.6 mmol) and CH_3I (125 μL , 2 mmol) were evenly stirred in DMSO (40 mL). The mixture solution was heated to 80 °C and agitated for 2 days. After that, the solution was cooled to 30 °C, adding excess CH_3I (1.00 g) to quaternize the remaining piperidine active sites. After reaction 1 day, the solution was precipitated in significantly extra EA (1 L) and purified with deionized water not less than 3 times to remove impurities. The yellowish powder was obtained by filtering and drying, and its yield was around 90%.

2.3. Membrane preparation

In 50 mL of DMSO, 1.00 g of the polyelectrolyte powder was added and stirred to get a clear solution. Then, the obtained solution was centrifuged to remove any insoluble solid and was cast onto a 25 cm² of square glass plate. After being dried at 80 °C for 24 h using a vacuum oven, a transparent and thin membrane (~15 μm) was peeled off carefully from the plate. Finally, the membrane samples were immersed in a 1 M NaOH solution for 48 h to fully exchange halide ion (I^- and Br^-) to OH^- and soaked in degassed purified water before measurements.

2.4. Characterization

The molecular structures of all synthesized materials including intermediate reactant and product crosslinkers, copolymer and polyelectrolytes were determined by a NMR spectrometer (Bruker, AV 400, Switzerland) using CDCl_3 , $\text{D}_2\text{O}/\text{CD}_3\text{OD}$ or/and DMSO-d₆ as the solvent. The analysis of the membrane morphology was realized by SEM (SEM, ZEISS Sigma, Germany), AFM (Bruker, USA), TEM (Tecnai F30, Japan) as well as SAXS (SAXSess mc², Austria). The specific operation methods

including sample preparation and test conditions are referred to our previous work [34].

2.5. Measurements

The typical property measurements, including ion exchange capacity (IEC), water uptake (WU), swelling ratio (SR), hydration number (λ), static water contact angle (SWCA), hydroxide conductivity, normalized ion diffusion coefficient (D/D_0), mechanical properties, and thermal and alkaline stability, are detailed in the SI. The QBNTP and dual-methylpiperidinium crosslinked poly(binaphthyl-co-terphenyl piperidinium) (QBNTP-MP11) AEMs were chosen for the fuel cell test. A well dispersed catalyst ink, containing a Pt/C catalyst (Hispec 4000, 40% Pt), a 5 wt% QAPBP/DMSO solution [26], isopropyl alcohol and deionized water (10:1 vol%), was sprayed onto both membranes using Exacta Coat OP3. The Pt-metal loadings at the cathode and the anode were controlled at $0.35 \pm 0.03 \text{ mg cm}^{-2}$. The coated membranes were separately sandwiched between two pieces of carbon paper to form two membrane electrode assemblies (MEAs). A fuel cell system (850E-100 W, Hephas Energy, China) was adopted to evaluate the fuel cell performance at 80 °C with a H₂/O₂ flow rate of 600 mL min⁻¹ and 100% RH without backpressure. The in-build impedance analyzer was used to record the high frequency resistance (HFR) of the two cells. Besides, the performance of the QBNTP-MP11 (25 μm) and QBNTP (25 μm) AEMs for water electrolysis was also considered. Pt/C and IrO₂ were used as the anode catalyst and the cathode catalyst, respectively. The catalyst loadings were controlled at 1 mg cm⁻² for both the electrodes and the active area was 4 cm². QAPBP was used as an anion exchange ionomer (AMI). The MEA prepared by the hot-pressed method was assembled into a water electrolysis cell. The polarization curve was collected at 80 °C by the voltage sweep method, and the potential was increased at a rate of 5 mV s⁻¹. The durability was evaluated at 80 °C by feeding a 1 M aqueous KOH solution into both the electrodes at a flow rate of 3 mL min⁻¹ and applying a constant current density of 1 A cm⁻².

2.6. Density functional theory (DFT) calculation

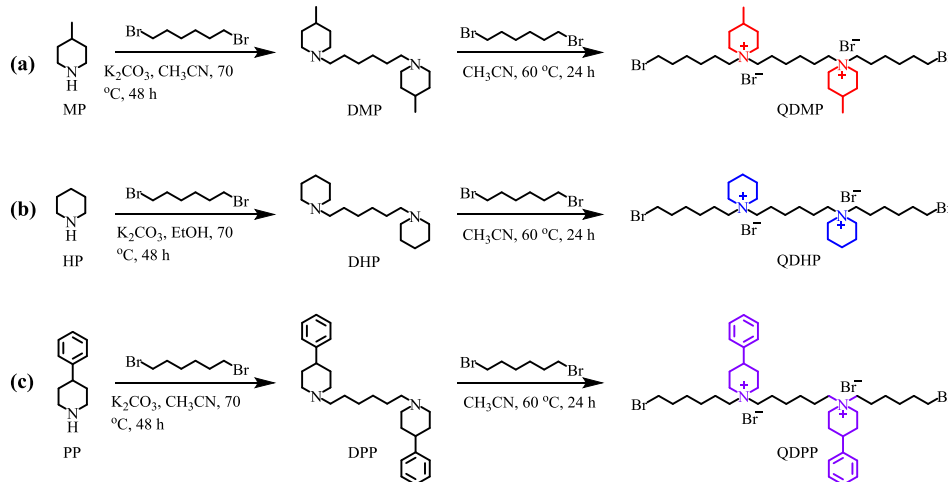
The optimized geometry structure, molecular orbital (MO) energy and Mulliken population analysis of each piperidinium-based crosslinker repeating unit and binding energy barrier of each repeating unit with OH⁻ were calculated by DFT at the M062-X/6-311 + G (d, p) level on Gaussian package and visualized in Gaussian or Chem3D [35].

3. Results and discussion

3.1. Synthesis and alkaline stability of piperidinium-based crosslinkers

Three types of dual-piperidinium crosslinkers were designed to reveal the influence of the C4-substituted piperidinium cations on their alkaline stability. The QDMP, QDHP and QDPP crosslinkers were synthesized according to the literature [33]. The specific synthesis procedures, as well as reaction conditions, are illustrated in Scheme 1(a – c). The ¹H NMR spectra of the reactant, intermediate and final crosslinkers are depicted in Figs. S1, S2 and S3. All the characteristic peaks were carefully assigned and labeled on the corresponding NMR spectra. The results show that all the desired dual-cation compounds (QDMP, QDHP and QDPP) were successfully synthesized by analyzing the change in the signal location and integral area of the ¹H NMR spectra.

To assess the influence of the C4-substituted piperidinium cations on their chemical stability, all the crosslinkers were treated in 5 M NaOH D₂O/CD₃OD (1:3 vol%) at 80 °C. Herein co-solvent CD₃OD plays a role in accelerating the cation degradation and facilitating the dissolution of the crosslinkers [33]. Throughout the test, all the solutions are always homogeneous and transparent. The structure of these compounds was elucidated with ¹H NMR spectroscopy (Fig. 1(a – c)). Several new signals appeared in the corresponding spectra, indicating that degradation occurred during the monitoring period. According to the ¹H NMR spectrum analysis, additional degradation peaks appeared at 2.0–3.5 ppm, indicating that these dual-cation crosslinkers may have degraded via S_N2 reaction, in which OH⁻ ions attack the α -C atoms on the dual-cation crosslinkers. Possibly because the α -C atoms directly connected to the N atom exhibit a more centralized positive distribution than the distant β -C atoms, implying that the nucleophile (OH⁻) can more easily attack the α -C atoms [20]. The degradation degree of the cation compounds was calculated by the integral-area ratio of their characteristic peaks [17]. As shown in Fig. 1(d), both QDMP and QDHP showed only 3.7% and 4.2% degradation, respectively, after 480 h of exposure in a 5 M NaOH D₂O/CD₃OD (1:3 vol%) solution, whereas QDPP showed 10.5% degradation under the same conditions. The pristine piperidinium group without substituents possesses special constrained ring conformation and can partly withstand the OH⁻ attack. When electron-donating methyl groups appear on the C4-position of the piperidinium ring, the electron density of the functional group with positive charge further increases, effectively reducing the likelihood of OH⁻ attack and greatly improving the alkaline stability of the piperidinium cation [17,36]. On the contrary, including electron-withdrawing phenyl substituent in the piperidinium ring can promote the cation degradation attacked by OH⁻ resulting in a decrease in the chemical stability. The



Scheme 1. Synthesis routes for piperidinium-based crosslinkers: (a) QDMP, (b) QDHP, and (c) QDPP.

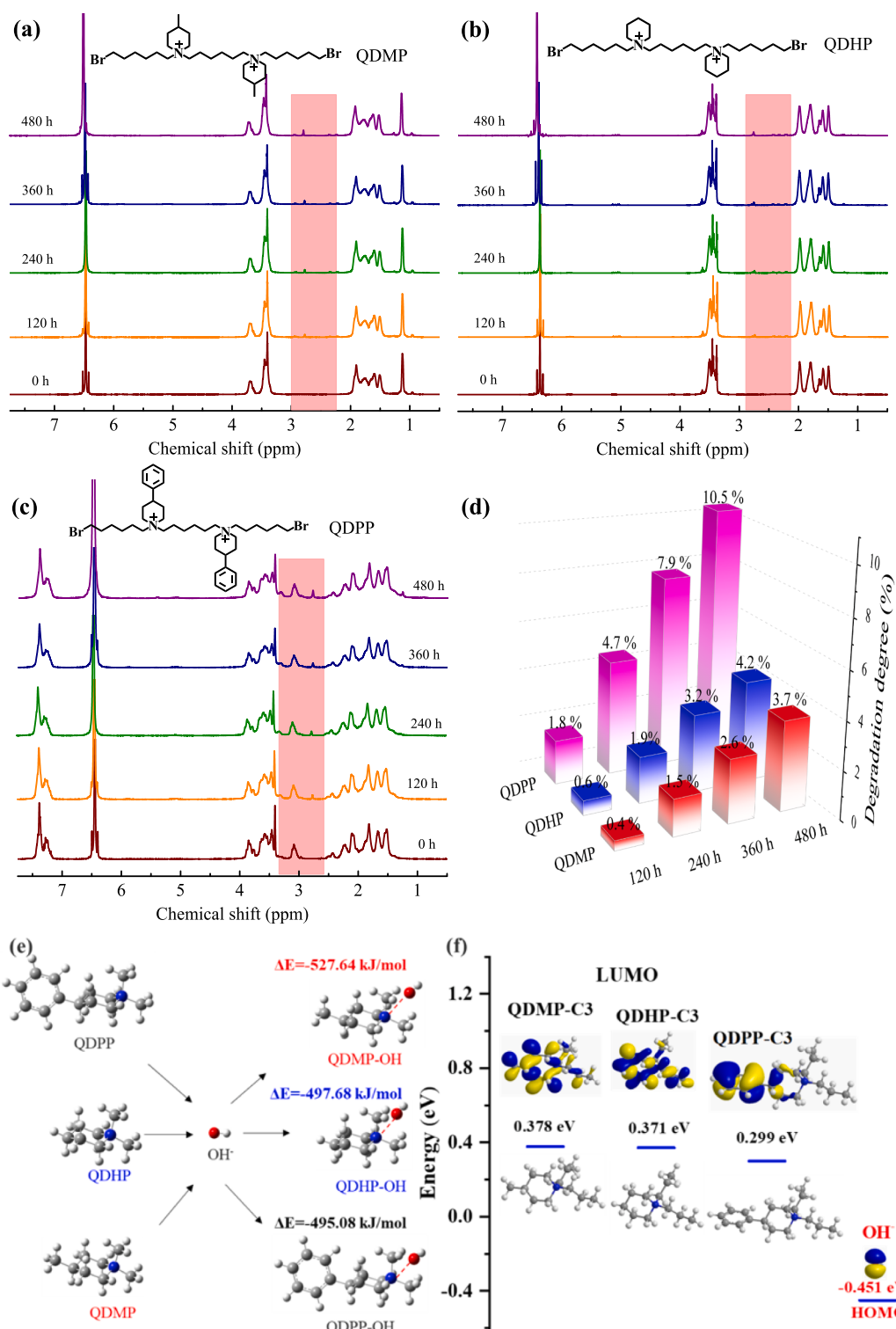


Fig. 1. ^1H NMR spectra of (a) QDMP, (b) QDHP and (c) QDPP in 5 M NaOH $\text{D}_2\text{O}/\text{CD}_3\text{OD}$ (1:3 vol%) at 80°C , (d) degradation degree of the resulted piperidinium-based crosslinkers in the alkaline stability test, (e) binding energy of the QDMP, QDHP and QDPP units with OH^- , and (f) molecular orbital energy of QDMP-C3, QDHP-C3, QDPP-C3 and OH^- in a water phase (yellow is positive and blue is negative). (For interpretation of the references to colour in this figure legend, the reader is referred to the web version of this article.)

alkaline stability of these piperidinium-based crosslinkers herein can be ranked as QDMP > QDHP > QDPP, and is in good accord with the report [1].

The binding energy barrier (ΔE) of the piperidinium cation repeating units with OH^- was calculated using DFT calculations. As displayed in

Fig. 1(e), the ΔE of QDMP-OH, QDHP-OH and QDPP-OH is -527.64 , -497.68 and $-495.08 \text{ kJ mol}^{-1}$, respectively. It means that the energy required for OH^- to bind the QDMP cation group is higher than that required for the other two piperidinium cation groups; and the OH^- groups are more susceptible to dissociation and transport between

adjacent QDMP groups, thus reducing the potential OH^- attack and improving its alkaline stability [37,38].

The molecular orbital (MO) energy of the crosslinker repeating units (cation with 2 $-\text{CH}_2\text{CH}_2-$ spacers, denoted as QDMP-C3, QDHP-C3 and QDPP-C3) in water phase is shown in Fig. 1(f). Notably, QDMP-C3 posed the highest LUMO energy of 0.378 eV among QDHP-C3 (0.371 eV), QDPP-C3 (0.299 eV), and HOMO energy of OH^- (-0.451 eV). This reveals that QDMP-C3 can be less susceptible to the OH^- attack than the other two crosslinkers, which is favored by the higher binding energy of QDMP with OH^- ions. All of these computational results perfectly align with the experimental results, emphasizing the QDMP robust alkaline stability. Furthermore, the Mulliken population analysis of the aforementioned symmetric piperidinium cations with three alkyl groups is depicted in Fig. S4. As can be observed, the α -C atoms directly connected to the N atom are positively charged while the β -C atoms separated from the N atom by one alkyl spacer are negatively charged. Notably, the charge distribution on the α -C atoms in the piperidinium ring is greater than that on the α -C atoms in the alkyl chains. This implies that the positively charged positions are more vulnerable to OH^- attack originating from the α -C atoms on the piperidinium ring, better known as $\text{S}_{\text{N}}2$ reaction [33]. Thus, it inspired us to map the possible degradation mechanism of these piperidinium cations under high-pH conditions (Fig. S5).

3.2. Synthesis and structural characterization of polymers

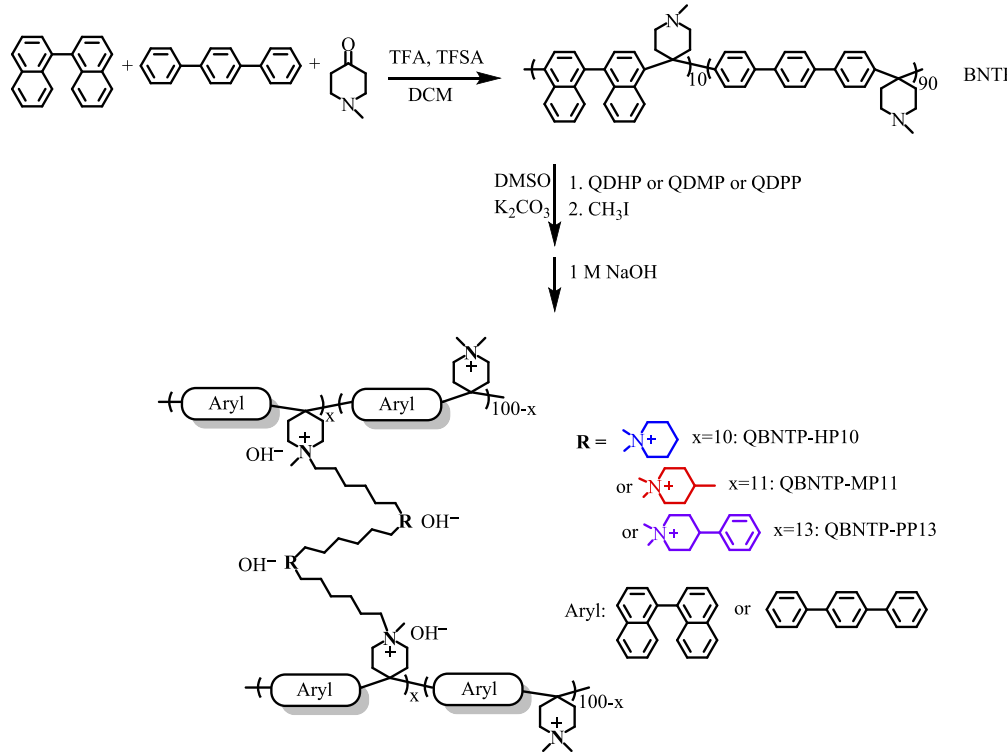
The ether-free BNTP copolymer was prepared via acid-catalyzed polycondensation, and the aryl to carbonyl compound feed ratio was fixed at 1.0:1.1 (mol%) to accelerate the polymerization and increase the polymer molecular weight [39]. During the process, the carbonyl group in 1-methyl-4-piperidone was firstly protonated by TFSAs to form electrophiles and then rapidly reacted with nucleophilic BN and TP aromatic monomers (1:9 mol%) via an electrophilic substitution, as indicated in Scheme 2. For the preparation of NMR samples, a few TFA (50 μL) was used as a co-solvent for the convenience of NMR analysis by splitting the protonated piperidine signals and shifting the water signal

[25]. As depicted in the ^1H NMR spectra of the BNTP copolymer (Fig. S6), the signals of 8.40–7.22 ppm are attributed to the aromatic protons whereas the signals of 3.70–2.10 ppm belong to the alkyl protons in the piperidine ring, indicating that the BNTP copolymer was successfully synthesized.

Different piperidinium-based crosslinked AEMs were prepared to study the influence of the C4-substituted piperidinium-based crosslinker on the morphology and property of the AEMs. All the desired polyelectrolytes were fabricated by a Menshutkin reaction with their corresponding dual-piperidinium compound or iodomethane (CH_3I) and the BNTP polymer backbone [32]. The molecular architectures of the resulted polyelectrolytes were clarified by ^1H NMR (Fig. S7(a–d)). The fully quaternized QBNTP was designed for comparison and its successful synthesis was confirmed by the relative integral area ratio between the piperidinium chemical shifts (2.3–2.2 ppm) and the aromatic chemical shifts (7.3–7.9 ppm) in Fig. S7(a). For the crosslinked polyelectrolytes: QBNTP-HP10, QBNTP-MP11 and QBNTP-PP13 (dual-phenyl-piperidinium crosslinked QBNTP), the last two digits denote the crosslinking degree (%). Herein the crosslinking degrees of the crosslinked AEMs were controlled in between 10%–13% determined by the integral ratio of aliphatic-H (1.1–1.8 ppm) to aromatic-H (7.2–7.9 ppm) in the ^1H NMR spectra of the corresponding crosslinked polyelectrolyte (Fig. S7(b–d)). Due to onset of gelation of the polyelectrolyte with 15% of crosslinking degree, a relatively low crosslinking degree range was thus imposed in this work to ensure the solubility of all the crosslinked polyelectrolytes and for the convenience of membrane preparation.

3.3. Morphological features

All the AEMs prepared by the solvent-casting method are transparent and flexible (Fig. S8(a)). All the resultant AEMs exhibited smooth and dense surface and could be controlled at a thickness of around 15 μm observed by SEM shown in Fig. S8(b and c)). Nanoscale phase separation is an effective method to promote the OH^- transport by building well-developed ionic highways. The microphase structure of the AEMs was explored by AFM. From the phase images shown in Fig. 2(a), the bright



Scheme 2. Synthesis of various dual-piperidinium crosslinked polyelectrolytes.

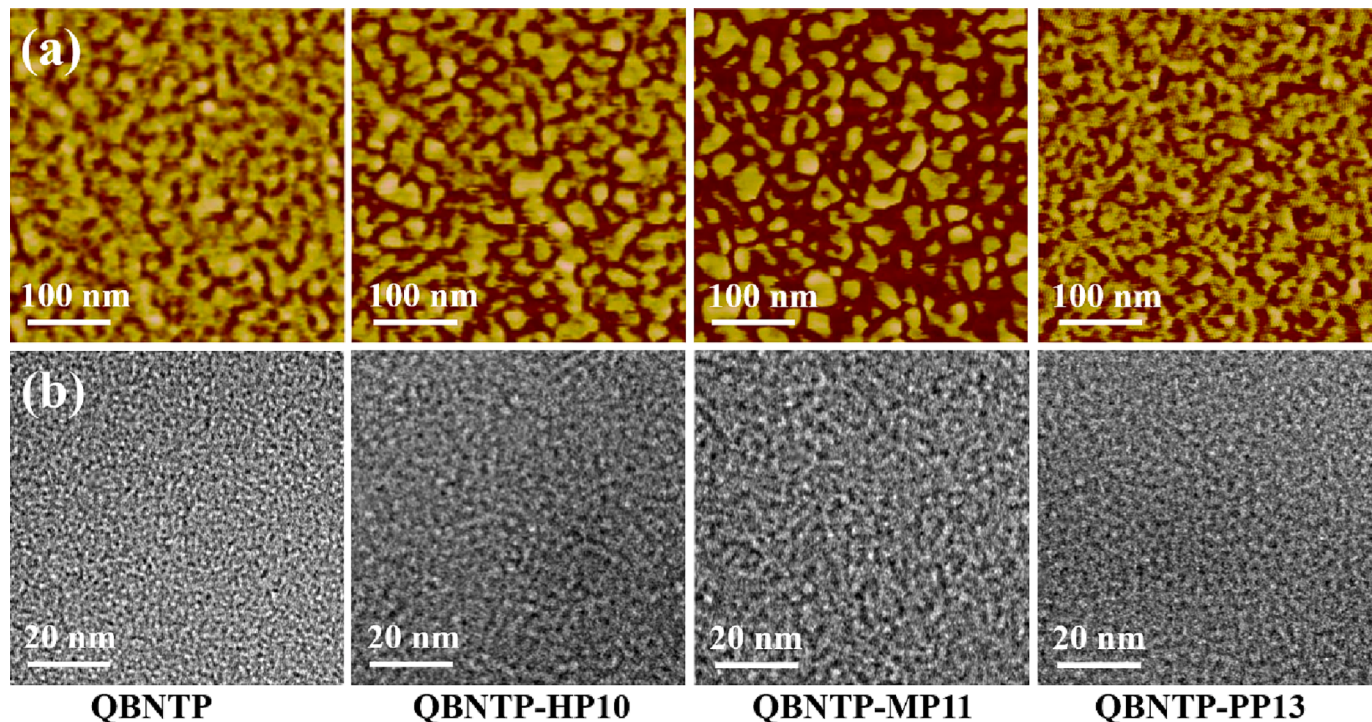


Fig. 2. The images of (a) AFM and (b) TEM of the as-prepared AEMs.

domains belong to the hydrophobic polymer framework while the dark domains denote the hydrophilic ionic clusters of the piperidinium cations. The crosslinked AEMs have an observably clearer hydrophilic/hydrophobic phase-separated morphology than the original QBNTP AEM ascribed to the existence of hydrophilic cation crosslinkers. It is noteworthy that the QBNTP-PP13 AEM shows smaller hydrophilic phase domains than the other two crosslinked AEMs, which is mainly attributed to the sterically bulky phenyl substituent in QBNTP-PP13 effectively preventing the agglomeration of the hydrophilic cation groups [40]. On the contrary, QBNTP-MP11 presents a marked phase separation morphology.

Meanwhile, TEM was also adopted to interpret the intramembranous nanophase morphology (Fig. 2(b)). The bright regions represent the hydrophobic aromatic polymer main chains whereas the dark regions signify the hydrophilic cationic clusters as anion conductors. By comparing all the as-prepared AEMs in this work, it is found that QBNTP-MP11 displays a clearest nanophase separation morphology forming large ion clusters and well-continuous ion conductive channels. This result is consistent with the AFM's (Fig. 2(a)). SAXS was employed to characterize the microstructure of the resulting AEMs as it can quantify and directly reflect ion-cluster size. As displayed in Fig. S9, the scattering vector of the as-resulted AEMs is detected at $0.35\text{--}0.39\text{ nm}^{-1}$. By utilizing the Bragg equation ($d = 2\pi/q_{\max}$), the values of the domain size (d) range in between 16.5 and 18.0 nm. The QBNTP-MP11 AEM possesses the lowest scattering peak position value and the most significant domain size, implying that QBNTP-MP11 has a larger hydrophilic domain than the other AEMs, as determined by the morphological analysis of TEM and AFM (Fig. 2).

3.4. Fundamental properties

Membranes with adequate IECs and good swelling resistance are the key for high efficiency and long-term lifetime of AEMFCs. As listed in Table 1, herein the as-fabricated AEMs possess a high IEC ($>2.70\text{ meq g}^{-1}$) measured by the back-titration method, which is close to the theoretical values (IEC: $2.78\text{--}2.90\text{ meq g}^{-1}$) obtained by ^1H NMR. The crosslinked AEMs display slightly higher IEC values than QBNTP owing

Table 1
Fundamental properties of the membranes.

Membrane	IEC (meq g ⁻¹)		WU (%)	SR (%)	λ	ρ (g cm ⁻³)	SWCA (°)
	Theo. ^a	Exp. ^b					
QBNTP	2.78	2.71 ± 0.07	45.2 ± 0.7	16.1 ± 0.2	9.0	1.52	83.1
QBNTP-HP10	2.90	2.82 ± 0.04	53.4 ± 0.5	12.8 ± 0.1	10.3	1.63	67.0
QBNTP-MP11	2.90	2.85 ± 0.06	59.4 ± 0.6	13.8 ± 0.3	11.4	1.71	61.1
QBNTP-PP13	2.87	2.84 ± 0.08	50.9 ± 0.6	7.5 ± 0.3	9.9	1.58	74.7

a. Calculated from NMR spectra of the AEMs with OH⁻.

b. Determined by back titration in OH⁻ form.

to the contribution of the dual-piperidinium crosslinkers. Moreover, all the resulted AEMs exhibit a moderate water uptake (WU) (67%–83%) combined with a limited swelling ratio (SR) (12%–22%) at 90 °C (Fig. S10(a and b)). The higher WU and lower SR of the crosslinked AEMs than those of the pristine QBNTP demonstrate that the introduction of piperidinium-based crosslinkers is beneficial for enhancing the water-retention ability and limiting the swelling of the AEMs by forming hydrophilic crosslinked networks [30]. Interestingly, QBNTP-MP11 showed a slightly higher WU than QBNTP-HP10, maybe the methyl substituent retarded the chain stacking and enlarged the interchain spacing, resulting in an enhanced water uptake, which is in line with the literature [41]. It should be noted that the QBNTP-PP13 AEM showed the lowest WU and SR, which indicated that the hydrophobic phenyl substituent group on the piperidinium cations could reduce the water uptake, leading to a slight dimensional change of QBNTP-PP13 in water [42]. Besides, the hydration number (λ) of all the AEMs is maintained at 9.0–11.4, and the density (ρ) of the as-prepared AEMs is in between 1.52 and 1.71 g cm⁻³ at 30 °C. The static water contact angle (SWCA) of all

the AEMs is in a range $61.1\text{--}83.1^\circ$, indicating that all the AEMs are generally hydrophilic. QBNTP-PP13 showed a higher value of SWCA than the other two crosslinked AEMs due to the presence of hydrophobic phenyl substituent in the crosslinker.

3.5. Mechanical properties and thermal stability

The long-term viability of applications in alkaline fuel cells or water electrolysis is in some way relied on the mechanically tough and thermally stable AEMs. As shown in Fig. 3(a), herein the as-resulted AEMs in OH^- form exhibit an excellent tensile strength (TS) ($30.1\text{--}31.0 \text{ MPa}$) and an acceptable elongation at break (Eb) ($11.1\%\text{--}24.6\%$). The crosslinked AEMs displayed a higher Eb ($>15.6\%$) than the pristine QBNTP counterpart ascribed to the incorporation of the flexible dual-piperidinium crosslinkers suggesting that these dual-cation crosslinkers can effectively improve the membrane toughness. QBNTP-MP11 showed the highest Eb among the three types of crosslinked AEMs, likely due to the higher WU value, inducing the softening of the membrane [43]. Besides, QBNTP-MP11 showed a superior toughness (implying both strong and flexible) with a value of 6.08 MJ m^{-3} to QBNTP-HP10 (3.72 MJ m^{-3}), QBNTP-PP13 (3.66 MJ m^{-3}) and QBNTP (2.44 MJ m^{-3}) (Fig. 3(b)). Moreover, to further explore the mechanical robustness of the resultant membranes, rheological measurements were implemented, as depicted in Fig. S11. All the as-prepared membranes exhibited an excellent storage modulus (G') and loss modulus (G'') in the range of $10^5\text{--}10^7 \text{ Pa}$.

In particularly, QBNTP-MP11 exhibits the highest average G' value of $6.52 \times 10^6 \text{ Pa}$. This is significantly higher than the G' values of QBNTP-HP10 ($1.88 \times 10^5 \text{ Pa}$), non-crosslinked QBNTP ($2.28 \times 10^5 \text{ Pa}$), and QBNTP-PP13 ($3.18 \times 10^5 \text{ Pa}$), by 3.5 times, 2.9 times, and 2 times its value, respectively. The attractive modulus of QBNTP-MP11 is mainly attributed to its flexible methyl moiety on the piperidinium group of the crosslinker and the impressive crosslinked structure. Overall, the as-prepared AEMs exhibit a satisfactory viscoelasticity and meet the mechanical property requirements for AEMFC [44]. It also can be seen from Fig. 3(c) that QBNTP-MP11 displayed an excellent flexibility and toughness as reflected by its folding ability and its capability of withstanding a weight 10,000 times its own weight.

Fig. 3(d and e) shows the TGA and DTG curves of the as-prepared AEMs. All the AEMs possess a good thermostability below 240°C , then the degradation of piperidinium cations between 240 and 350°C , and final breakage of the polymer backbones at 520°C . Slight decomposition before 100°C observed in the DTG curve (Fig. 3(e)) might be caused by moisture absorption from the air during weighing. It should be noted that QBNTP-PP13 showed higher degradation temperature than other membranes at each thermal decomposition stage, possibly originating from the thermally stable phenyl substituent in the crosslinker [45,46].

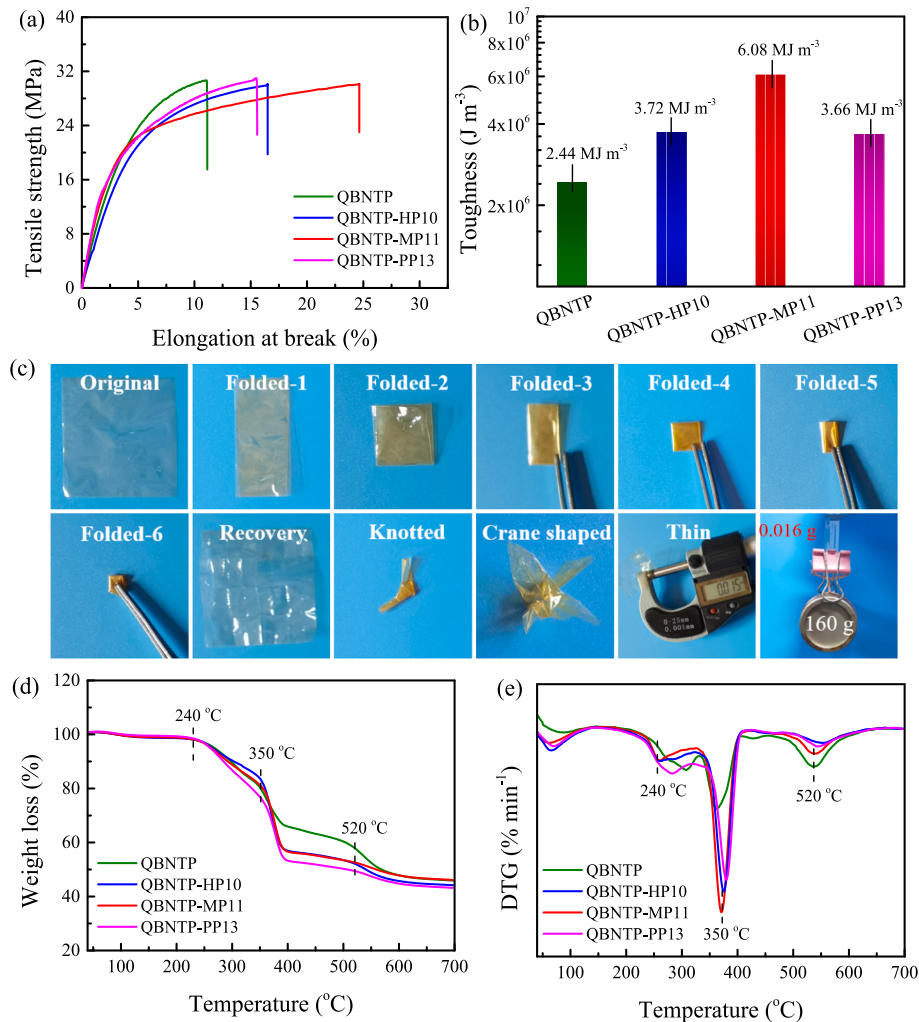


Fig. 3. The (a) mechanical property and (b) toughness of the AEMs, (c) physical display diagram of the mechanical toughness of QBNTP-MP11, and (d) TGA and (e) DTG curves of the as-prepared AEMs.

3.6. Ion transport properties

Ion transport properties are one of the most critical parameters of AEMs and significantly dictate the power output performance and their applications. As shown in Fig. 4(a), the crosslinked AEMs have the OH⁻ conductivities superior to the native QBNTP attributed to higher IEC and WU for the former. Among the three types of crosslinked AEMs, QBNTP-MP11 exhibited the highest OH⁻ conductivity (181.2 mS cm⁻¹ at 90 °C) ascribed to a distinct nanophase separation and higher WU, while QBNTP-PP13 showed an inferior OH⁻ conductivity at the same temperature as a result of its lower WU from the inherent hydrophobic nature of the benzene ring on the piperidinium-cation crosslinker. These results matched well with the morphology observations (Fig. 2). Additionally, the apparent activation energy (E_a) calculated by the Arrhenius equation ($E_a = -bR$, where b is the slope and R is the ideal-gas constant) is plotted in Fig. 4(b), and the E_a values of all the resulted membranes are in 20.01–20.66 kJ mol⁻¹, reflecting a low energy barrier confronted by anion transport. The higher conductivity of QBNTP-MP11 may stem from higher IEC combined with WU and better phase separation, not just from single one of them. Whereas the higher E_a value of QBNTP-MP11 is probably ascribed to the introduction of a more hydrophilic QDMP-based crosslinker, suggesting that varying the crosslinker structure and water uptake may have a potential effect on the temperature dependent conductivity [47–49]. Fig. 4(c) shows the OH⁻ conductivity-modulus relationship of the resulted AEMs at a temperature in between 30 and 90 °C. Of these, with the highest OH⁻ conductivity and the highest modulus, QBNTP-MP11 is superior to the other as-prepared AEMs, indicating that QBNTP-MP11 has the “win-win” merit of high mechanical strength and ionic conductivity.

Furthermore, Fig. 4(d) shows the conductivity and SR of some representative crosslinked AEMs with ether-free polyaromatic main chains in current study and in other publications for comparison [31,32,50–55]. Meanwhile Table S1 lists the IEC, WU, SR and conductivity of some crosslinked poly(arylene)-based AEMs. All the piperidinium-based crosslinked AEMs in the present study demonstrate a superior hydroxide conductivity with slight dimensional swelling, making them promising materials for FCs. Ultimately, a normalized ion diffusion coefficient (D/D_0) was measured for a further understanding of

the intrinsic ionic conductivity of the AEMs. Fig. 4(e) shows the D/D_0 values of the as-prepared AEMs herein and some currently reported AEMs [34,56–59]. The AEMs in this work have higher D/D_0 values (at a relatively low λ level) than some membranes reported in the literature [34,56–59]. The high D/D_0 value of QBNTP-MP11 disclosed its fast ion transport properties, resulting in a superb OH⁻ conductivity. This can be explained by the distinct nanophase separation as well as well-developed ionic highways within the QBNTP-MP11 AEM. (as verified by morphological analysis).

3.7. Alkaline stability

Chemically stable AEMs can provide powerful guarantee for long-term operation of AEMFCs or AEMWE. Variations in the conductivity and molecular architecture of the AEMs under a strong basic environment and at elevated temperature can well reflect their chemical stability. As enunciated in Fig. 5a, the conductivity loss of all the membranes is less than 10% monitored by immersing them in 2 M NaOH at 80 °C for 1560 h. The lower conductivity loss of the crosslinked AEMs might be due to the steric shielding of the piperidinium-based crosslinkers with flexible alkyl chains, thereby increasing the difficulty of OH⁻ attack on the cationic groups. After the rigorous alkaline stability test, the crosslinked QBNTP-MP11 AEM proclaimed an outstanding alkaline stability with less than 5% loss of the OH⁻ conductivity. According to the aforesaid experimental and theoretical results, QBNTP-MP11 is the most stable membrane derived from the excellent alkaline resistance of the electron-donating substituent QDMP [1,36].

Furthermore, the ¹H NMR spectra of all the membranes before and after the alkaline test can gain an insight into the structure breakdown. As shown in Fig. 5(b) and Fig. S12(a-c), all the ¹H NMR spectra exhibit negligible signals from the degradation of piperidinium cations in the prepared AEMs after 1560 h. This indicates an unobvious degeneration of the molecular architecture of membranes during the test. On one hand, the backbone without alkali-sensitive heteroatoms and aromatic-ether bonds guarantees a good alkaline resistance under a harsh alkaline environment. On the other hand, the highly durable dual-piperidinium crosslinkers can also further reinforce the durability of AEMs by providing conformational protections. Therefore, these results assert

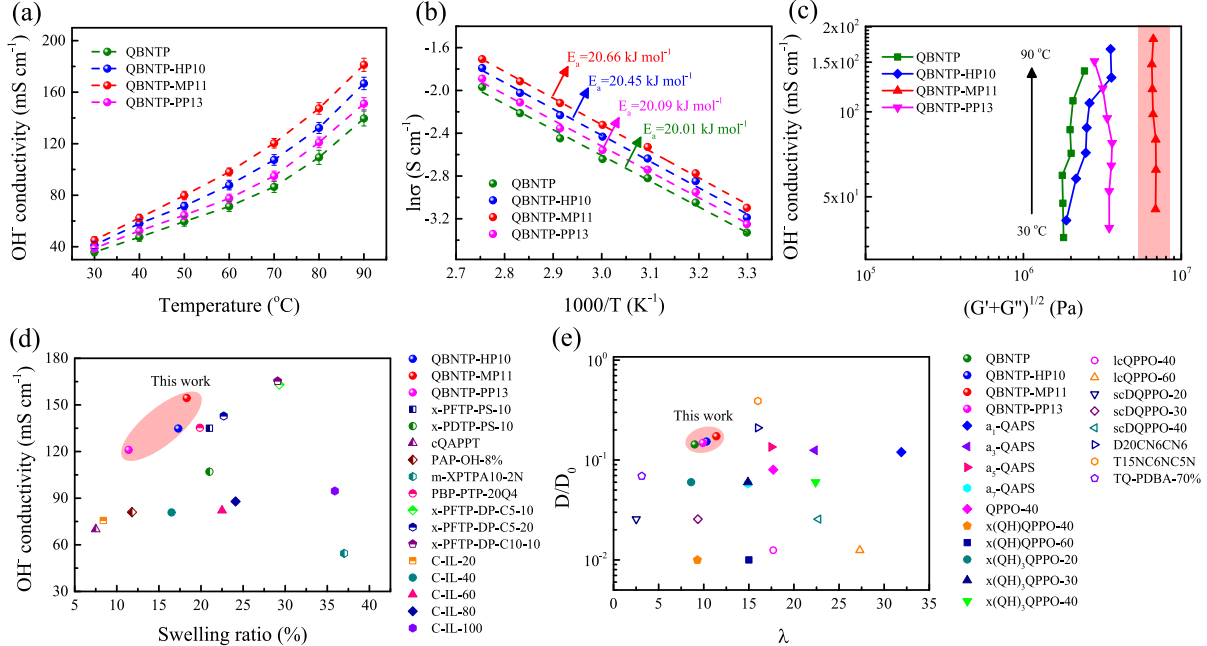


Fig. 4. (a) OH⁻ conductivity, (b) Arrhenius plots and (c) conductivity-modulus relationship of the resulted AEMs, (d) conductivity as a function of SR of the AEMs in this work and in the literature [31,32,50–55], and (e) comparison of D/D_0 of the as-prepared AEMs with other reports [34,56–59].

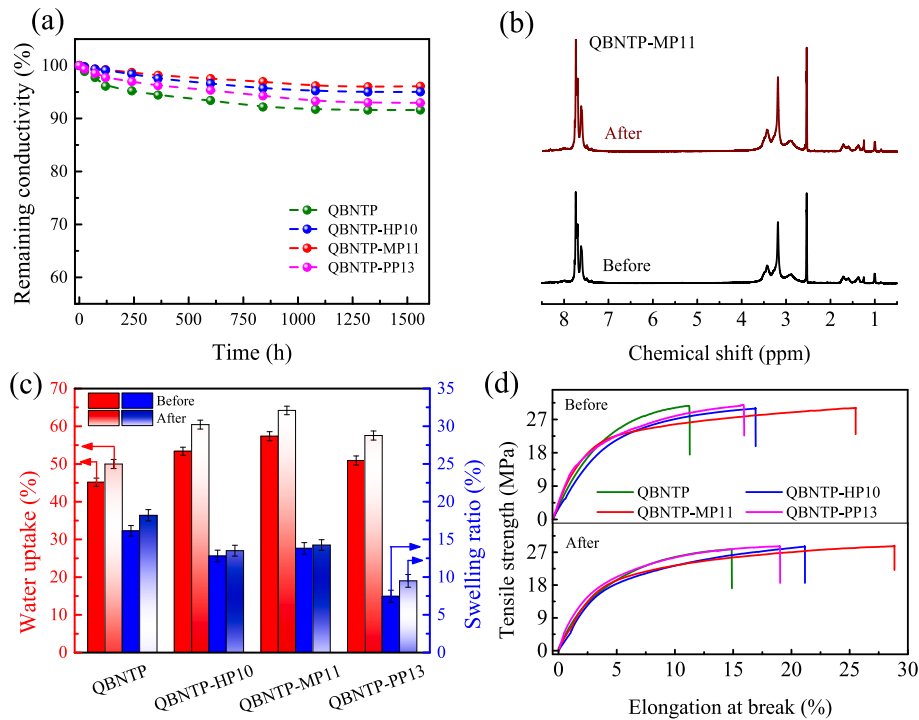


Fig. 5. (a) Change of conductivity of the AEMs as a function of time during test, (b) ^1H NMR spectrum of QBNTP-MP11, (c) WU and SR, and (d) mechanical properties of the membranes before and after the alkaline test.

that the piperidinium-based crosslinked AEMs are promising to be an advanced material for AEMFCs or AEMWE.

Interestingly, all the membranes after the alkaline treatment preserve both higher WU and SR than before treatment (Fig. 5(c)). This

phenomenon is perhaps attributed to the effect of hydration-induced plasticization that amorphous polymers can unwind the chain entanglement during the long-time high temperature alkaline treatment, increasing the free volume for water storage and improving SR [43,60].

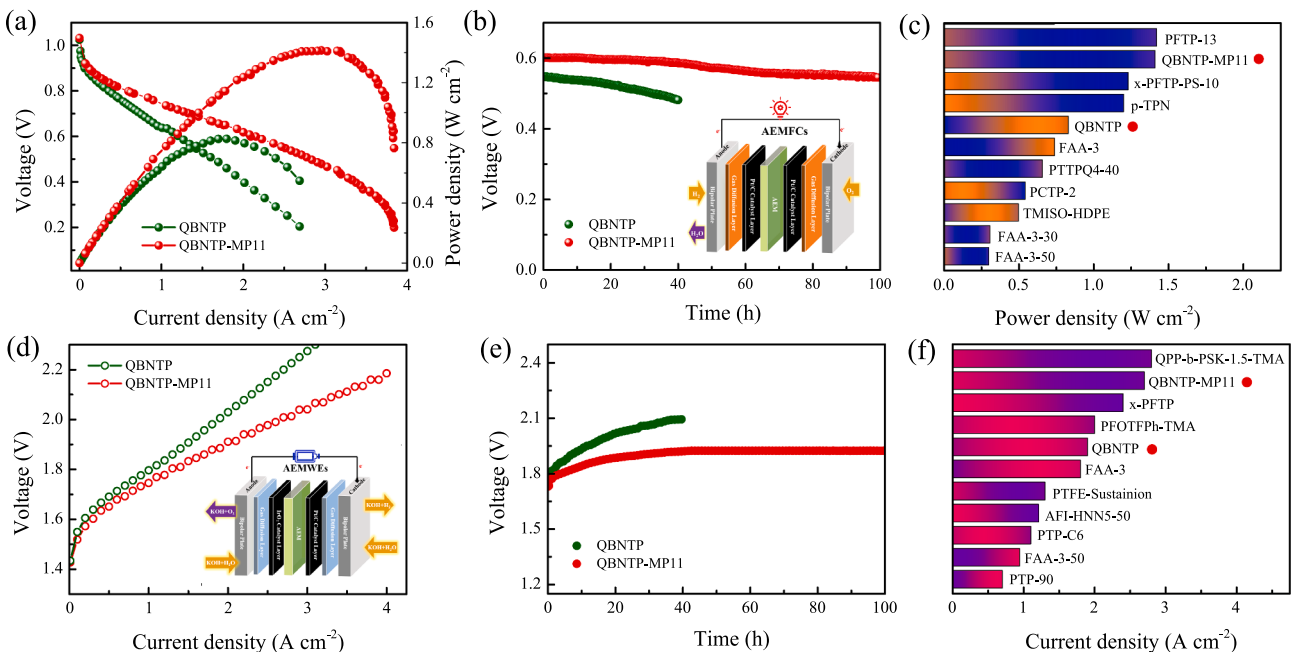


Fig. 6. (a) Polarization curves and power density of the fuel cell with the QBNTP and QBNTP-MP11 AEMs, (b) durability of AEMFC with QBNTP-MP11 and QBNTP at 80 °C, (c) comparison on PPD of a H_2/O_2 single cell in this work (a red circle) and in the reports in the past five years [24,28,50,64–68], (d) polarization curves for alkaline water electrolysis based on QBNTP-MP11 and QBNTP at 80 °C and ambient pressure by circulating a 1 M KOH solution in the anode and cathode at a rate of 3 mL min^{-1} . Test conditions: IrO_2 loadings of 1 mg cm^{-2} and 7.5 wt% QAPBP for anode; Pt/C loadings of 1 mg cm^{-2} and 25 wt% QAPBP for cathode, (e) durability of AEMWE with QBNTP-MP11 and QBNTP at 80 °C and a constant current density of 1 A cm^{-2} at ambient pressure, and (f) comparison on current density at 2.0 V for alkaline water electrolysis in this work (a red circle) and in current reports [67,69–75]. (For interpretation of the references to colour in this figure legend, the reader is referred to the web version of this article.)

This results in a depression in both membrane degradation by shielding layer of water and membrane mechanical stability, signifying that a reasonable water uptake is important for improving the alkaline stability of AEMs [61]. As shown in Fig. 5(d), the Eb of the AEMs increased while the TS decreased after the alkaline stability test mainly due to the increased water absorption resulting in less brittle and more rubbery AEMs [43]. This result further emphasizes that the AEMs possess an excellent mechanical durability even after being in service under high-pH conditions for 1560 h. A slight change in the water uptake can be observed after the alkaline test, likely resulting in acceptable variations of the conductivity, and dimensional and mechanical stability. For the effect of water content on the alkaline stability of AEMs, as noted by Dekel et al. [43,61–63], the cations degraded more rapidly with decreasing the water content, resulting in a decline in the membrane performance.

3.8. Potential applications

3.8.1. Fuel cell

The QAPBP ionomers, QBNTP and QBNTP-MP11 AEMs were assembled into fuel cell fixtures by the catalyst-coated membrane (CCM) method. Fig. 6(a) shows a high open circuit voltage (OCV) of over 1.00 V for both the cells. This manifests that both the AEMs can effectively block gas penetration. More importantly, the cell assembled with the crosslinked QBNTP-MP11 AEM signals an exceptional peak power density (PPD) of 1.41 W cm^{-2} at a current density of 3.18 A cm^{-2} at 80°C and 100% RH without back pressure. QBNTP-MP11 shows a much higher PPD value than QBNTP (0.83 W cm^{-2}) due to its higher ionic conductivity and toughness. Furthermore, the HFR of the two cells was collected and plotted, as shown in Fig. S13. The QBNTP-MP11 based cell unveiled a lower HFR ($0.06\text{--}0.04 \Omega \text{ cm}^2$) than QBNTP ($\sim 0.09 \Omega \text{ cm}^2$). The durability single cell with QBNTP or QBNTP-MP11 was examined at 80°C , 100% RH, 0.2 A cm^{-2} current density and H_2/O_2 flow rate of 200 mL min^{-1} . A slower voltage decay rate of 0.5 mV h^{-1} in 100 h can be found for the QBNTP-MP11-based cell, and a larger voltage decay rate of 2.0 mV h^{-1} in 40 h for the QBNTP-based cell (Fig. 6b). Moreover, the QBNTP-MP11-based cell displays a higher voltage retention ($>91\%$) after 100 h, indicating that QBNTP-MP11 is highly promising for AEMFC. The excellent durability may be attributed to the efficient ionic transport, robust mechanical strength and chemical stability of QBNTP-MP11. Fig. 6(c) shows the PPD of H_2/O_2 single cells based on the AEMs in this work and those reported in the past five years [24,28,50,64–68]. The QBNTP-MP11-based cell yields a PPD in a high level, and is superior to commercial FAA-3–50, FAA-3–30 and FAA-3 with the PPD value of 0.299 , 0.306 and 0.738 W cm^{-2} , respectively. The result implied that the crosslinked QBNTP-MP11 AEM is a hopeful material for AEMFC.

3.8.2. Water electrolysis

The QBNTP-MP11 and QBNTP AEMs were also applied for water electrolysis in a 1 M KOH solution. Pt/C, IrO₂ and QAPBP were utilized as the anode catalyst, the cathode catalyst and the AMI, respectively. Fig. 6(d) gives the polarization curves of MEA with QBNTP-MP11 or QBNTP at 80°C . Expectedly, the MEA assembled with QBNTP-MP11 generates a higher current density (2.7 A cm^{-2} at 2.0 V) than that with QBNTP (1.9 A cm^{-2} at 2.0 V), mainly ascribed to the enhanced conductivity of QBNTP-MP11 because of its low inner ohmic resistance. This result is in accord well with its single cell performance. In addition, the durability of QBNTP-MP11 and QBNTP in alkaline water electrolysis was evaluated by circulating a 1 M KOH electrolyte at a preset current density of 1 A cm^{-2} . The voltage of the QBNTP-MP11-based cell increased with a rate of 2.0 mV h^{-1} in 100 h under 1 A cm^{-2} current density at 80°C , while that of the QBNTP-based cell increased with a rate of 9.0 mV h^{-1} within 40 h under the same condition, as depicted in Fig. 6(e). This means that the cell with QBNTP-MP11 shows better water electrolysis performance and durability than that with QBNTP. According to a comparison of the polarized current density of AEMWE in

this work (Fig. 6(f)) and in current reports [67,69–75], the current density of the QBNTP-MP11-based MEA is at a substantially decent level and could be improved by optimizing the operating conditions. These findings reveal that the QBNTP-MP11 AEM has the potential to be used in alkaline water electrolysis.

4. Conclusions

To sum up, a series of dual-piperidinium crosslinkers was synthesized for the first time, and their alkaline stability was valued by both experiment and computation. Of those, the QDMP crosslinker with electron-donating groups exhibits a robust alkaline stability. By dual-cation crosslinking, the crosslinked AEMs are found to evince more obvious microphase separation as well as well-connected conductive nanochannels than the pristine QBNTP AEM. Among them, QBNTP-MP11 exhibits a remarkable OH^- conductivity of 181.2 mS cm^{-1} with a limited swelling ratio of 19.7% at 90°C . Meanwhile, QBNTP-MP11 shows striking mechanical properties including an impressive toughness (6.08 MJ m^3) and an excellent storage modulus ($6.52 \times 10^6 \text{ Pa}$). Furthermore, benefiting from the robust chemical stability of the QDMP crosslinker, QBNTP-MP11 possesses an outstanding alkaline stability, displaying an ionic conductivity retention $> 95\%$ after soaked in 2 M NaOH at 80°C for 1560 h. Notably, the single cell based on QBNTP-MP11 exhibits a high PPD of 1.41 W cm^{-2} at a current density of 3.18 A cm^{-2} at 80°C . The cell with QBNTP-MP11 manifests a high current density of 2.7 A cm^{-2} at 2.0 V and an acceptable durability in water electrolysis. Meanwhile, a decent durability of QBNTP-MP11 can be observed in the operation of AEMFC and AEMWE. All those results highlight the superior overall performance of QBNTP-MP11 with great potential for fuel cell and water electrolysis applications.

Declaration of Competing Interest

The authors declare that they have no known competing financial interests or personal relationships that could have appeared to influence the work reported in this paper.

Data availability

The authors do not have permission to share data.

Acknowledgments

We gratefully appreciate the financial support from the National Natural Science Foundation of China (Grant No. 22078272 & 22278340).

Appendix A. Supplementary data

Supplementary data to this article can be found online at <https://doi.org/10.1016/j.cej.2023.143107>.

References

- [1] N. Chen, Y. Jin, H. Liu, C. Hu, B. Wu, S. Xu, H. Li, J. Fan, Y.M. Lee, Insight into the alkaline stability of N-heterocyclic ammonium groups for anion-exchange polyelectrolytes, *Angew. Chem. Int. Ed.* 60 (2021) 19272–19280.
- [2] V. Vijayakumar, S.Y. Nam, Recent advancements in applications of alkaline anion exchange membranes for polymer electrolyte fuel cells, *J. Ind. Eng. Chem.* 70 (2019) 70–86.
- [3] J. Xue, J. Zhang, X. Liu, T. Huang, H. Jiang, Y. Yin, Y. Qin, M.D. Guiver, Toward alkaline-stable anion exchange membranes in fuel cells: cycloaliphatic quaternary ammonium-based anion conductors, *Electrochim. Energ. Rev.* 5 (2) (2022) 348–400.
- [4] D. Aili, A.G. Wright, M.R. Kraglund, K. Jankova, S. Holdcroft, J.O. Jensen, Towards a stable ion-solvating polymer electrolyte for advanced alkaline water electrolysis, *J. Mater. Chem. A* 5 (10) (2017) 5055–5066.

- [5] K. Chand, O. Paladino, Recent developments of membranes and electrocatalysts for the hydrogen production by anion exchange membrane water electrolyzers: a review, *Arabian J. Chem.* 16 (2023) 104451–104507.
- [6] E.J. Park, C.G. Arges, H. Xu, Y.S. Kim, Membrane strategies for water electrolysis, *ACS Energy Lett.* 7 (10) (2022) 3447–3457.
- [7] Z.F. Pan, L. An, T.S. Zhao, Z.K. Tang, Advances and challenges in alkaline anion exchange membrane fuel cells, *Prog. Energy Combust. Sci.* 66 (2018) 141–175.
- [8] G. Das, J.-H. Choi, P.K.T. Nguyen, D.-J. Kim, Y.S. Yoon, Anion exchange membranes for fuel cell application: a review, *Polymers* 14 (2022) 1197–1231.
- [9] A.M. Ahmed Mahmoud, K. Miyatake, Highly conductive and alkaline stable partially fluorinated anion exchange membranes for alkaline fuel cells: Effect of ammonium head groups, *J. Membr. Sci.* 643 (2022) 120072–120085.
- [10] X. Zhang, J. Guo, X. Chu, C. Fang, Y. Huang, L. Liu, N. Li, Mechanically flexible bulky imidazolium-based anion exchange membranes by grafting PEG pendants for alkaline fuel cells, *J. Membr. Sci.* 659 (2022) 120820–120831.
- [11] F. Gu, H. Dong, Y. Li, Z. Sun, F. Yan, Base stable pyrrolidinium cations for alkaline anion exchange membrane applications, *Macromolecules* 47 (19) (2014) 6740–6747.
- [12] J. Zhang, W. Yu, X. Liang, K. Zhang, H. Wang, X. Ge, C. Wei, W. Song, Z. Ge, L. Wu, T. Xu, Flexible bis-piperidinium side chains construct highly conductive and robust anion-exchange membranes, *ACS Appl. Energy Mater.* 4 (9) (2021) 9701–9711.
- [13] M. Kumari, J.C. Douglan, D.R. Dekel, Crosslinked quaternary phosphonium-functionalized poly(ether ether ketone) polymer-based anion-exchange membranes, *J. Membr. Sci.* 626 (2021) 119167–119179.
- [14] X. Liu, N. Xie, J. Xue, M. Li, C. Zheng, J. Zhang, Y. Qin, Y. Yin, D.R. Dekel, M. D. Guiver, Magnetic-field-oriented mixed-valence-stabilized ferrocenium anion-exchange membranes for fuel cells, *Nat. Energy* 7 (2022) 329–339.
- [15] W. You, K.M. Hugar, R.C. Selhorst, M. Treichel, C.R. Peltier, K.J.T. Noonan, G. W. Coates, Degradation of organic cations under alkaline conditions, *J. Org. Chem.* 86 (1) (2021) 254–263.
- [16] T. Zhu, Y.e. Sha, H.A. Firoozjaie, X. Peng, Y. Cha, D.M.M.M. Dissanayake, M. D. Smith, A.K. Vannucci, W.E. Mustain, C. Tang, Rational synthesis of metallo-cations toward redox- and alkaline-stable metallo-polyelectrolytes, *J. Am. Chem. Soc.* 142 (2) (2020) 1083–1089.
- [17] J. Fan, A.G. Wright, B. Britton, T. Weissbach, T.J.G. Skalski, J. Ward, T.J. Peckham, S. Holdcroft, Cationic polyelectrolytes, stable in 10 M KOH_{aq} at 100 °C, *ACS Macro Lett.* 6 (10) (2017) 1089–1093.
- [18] Z. Si, L. Qiu, H. Dong, F. Gu, Y. Li, F. Yan, Effects of substituents and substitution positions on alkaline stability of imidazolium cations and their corresponding anion-exchange membranes, *ACS Appl. Mater. Interfaces* 6 (6) (2014) 4346–4355.
- [19] J. Pan, Z. Sun, H. Zhu, H. Cao, B. Wang, J. Zhao, F. Yan, Synthesis and characterization of main-chain type polyimidazolium-based alkaline anion exchange membranes, *J. Membr. Sci.* 610 (2020) 118283–118294.
- [20] J. Li, C. Yang, S. Wang, Z. Xia, G. Sun, Chemically stable piperidinium cations for anion exchange membranes, *RSC Advances* 12 (41) (2022) 26542–26549.
- [21] W. You, K.J.T. Noonan, G.W. Coates, Alkaline-stable anion exchange membranes: a review of synthetic approaches, *Progre. Polymer Sci.* 100 (2020) 101177–101190.
- [22] J. Wang, Y. Zhao, B.P. Setzler, S. Rojas-Carbonell, C. Ben Yehuda, A. Amel, M. Page, L. Wang, K. Hu, L. Shi, S. Gottesfeld, B. Xu, Y. Yan, Poly(aryl piperidinium) membranes and ionomers for hydroxide exchange membrane fuel cells, *Nat. Energy* 4 (2019) 392–398.
- [23] N. Chen, C. Hu, H.H. Wang, S.P. Kim, H.M. Kim, W.H. Lee, J.Y. Bae, J.H. Park, Y. M. Lee, Poly(alkyl-terphenyl piperidinium) ionomers and membranes with an outstanding alkaline-membrane fuel-cell performance of 2.58 W cm⁻², *Angew. Chem. Int. Ed.* 133 (2021) 7789–7797.
- [24] N. Chen, H.H. Wang, S.P. Kim, H.M. Kim, W.H. Lee, C. Hu, J.Y. Bae, E.S. Sim, Y.-C. Chung, J.-H. Jang, S.J. Yoo, Y. Zhuang, Y.M. Lee, Poly(fluorenyl aryl piperidinium) membranes and ionomers for anion exchange membrane fuel cells, *Nat. Commun.* 12 (2021) 2367–2379.
- [25] J.S. Olsson, T.H. Pham, P. Jannasch, Poly(arylene piperidinium) hydroxide ion exchange membranes: Synthesis, alkaline atability, and conductivity, *Adv. Funct. Mater.* 28 (2018) 1702758–1702768.
- [26] W.T. Gao, X.L. Gao, W.W. Gou, J.J. Wang, Z.H. Cai, Q.G. Zhang, A.M. Zhu, Q.L. Liu, High-performance tetracyclic aromatic anion exchange membranes containing twisted binaphthyl for fuel cells, *J. Membr. Sci.* 655 (2022) 120578–120588.
- [27] W.W. Gou, W.T. Gao, X.L. Gao, Q.G. Zhang, A.M. Zhu, Q.L. Liu, Highly conductive fluorinated poly(biphenyl piperidinium) anion exchange membranes with robust durability, *J. Membr. Sci.* 645 (2022) 120200–120211.
- [28] J.J. Wang, W.T. Gao, Y.S.L. Choo, Z.H. Cai, Q.G. Zhang, A.M. Zhu, Q.L. Liu, Highly conductive branched poly(aryl piperidinium) anion exchange membranes with robust chemical stability, *J. Colloid Interface Sci.* 629 (2023) 377–387.
- [29] H.H. Wang, C. Hu, J.H. Park, H.M. Kim, N.Y. Kang, J.Y. Bae, W.H. Lee, N. Chen, Y. M. Lee, Reinforced poly(fluorenyl-co-terphenyl piperidinium) anion exchange membranes for fuel cells, *J. Membr. Sci.* 644 (2022) 120160–120168.
- [30] N. Chen, C. Lu, Y. Li, C. Long, Z. Li, H. Zhu, Tunable multi-cations-crosslinked poly(arylene piperidinium)-based alkaline membranes with high ion conductivity and durability, *J. Membr. Sci.* 588 (2019) 117120–117129.
- [31] T. Zhao, C. Long, Z. Wang, H. Zhu, Multication cross-linked poly(p-terphenyl isatin) anion exchange membranes for fuel cells: Effect of cross-linker length on membrane performance, *ACS Appl. Energy Mater.* 4 (2021) 14476–14487.
- [32] N. Chen, J.H. Park, C. Hu, H.H. Wang, H.M. Kim, N.Y. Kang, Y.M. Lee, Di-piperidinium-crosslinked poly(fluorenyl-co-terphenyl piperidinium)s for high-performance alkaline exchange membrane fuel cells, *J. Mater. Chem. A* 10 (7) (2022) 3678–3687.
- [33] X. Tan, Z. Sun, J. Pan, J. Zhao, H. Cao, H. Zhu, F. Yan, Alkaline stable pyrrolidinium-type main-chain polymer: the synergistic effect between adjacent cations, *J. Membr. Sci.* 618 (2021) 118689–118699.
- [34] X.L. Gao, L.X. Sun, H.Y. Wu, Z.Y. Zhu, N. Xiao, J.H. Chen, Q. Yang, Q.G. Zhang, A. M. Zhu, Q.L. Liu, Highly conductive fluorine-based anion exchange membranes with robust alkaline durability, *J. Mater. Chem. A* 8 (26) (2020) 13065–13076.
- [35] M.J. Frisch, G.W. Trucks, H.B. Schlegel, G.E. Scuseria, M.A. Robb, J.R. Cheeseman, G. Scalmani, V. Barone, G.A. Petersson, H. Nakatsuji, X. Li, M. Caricato, A.V. Marenich, J. Bloino, B.G. Janesko, R. Gomperts, B. Mennucci, H.P. Hratchian, J.V. Ortiz, A.F. Izmaylov, J.L. Sonnenberg, Williams, F. Ding, F. Lipparini, F. Egidi, J. Goings, B. Peng, A. Petrone, T. Henderson, D. Ranasinghe, V.G. Zakrzewski, J. Gao, N. Rega, G. Zheng, W. Liang, M. Hada, M. Ehara, K. Toyota, R. Fukuda, J. Hasegawa, M. Ishida, T. Nakajima, Y. Honda, O. Kitao, H. Nakai, T. Vreven, K. Throssell, J.A. Montgomery Jr., J.E. Peralta, F. Ogliaro, M.J. Bearpark, J.J. Heyd, E.N. Brothers, K.N. Kudin, V.N. Staroverov, T.A. Keith, R. Kobayashi, J. Normand, K. Raghavachari, A.P. Rendell, J.C. Burant, S.S. Iyengar, J. Tomasi, M. Cossi, J.M. Millam, M. Klene, C. Adamo, R. Cammi, J.W. Ochterski, R.L. Martin, K. Morokuma, O. Farkas, J.B. Foresman, D.J. Fox Gaussian 16 Rev. B.01, Wallingford, CT, 2016.
- [36] J. Chen, M. Zhang, C. Shen, S. Gao, Preparation and characterization of non-n-bonded side-chain anion exchange membranes based on poly(2,6-dimethyl-1,4-phenylene oxide), *Ind. Eng. Chem. Res.* 61 (4) (2022) 1715–1724.
- [37] Q. Liu, W. Ma, L. Tian, J. Li, L. Yang, F. Wang, Z. Wang, J. Li, Z. Wang, H. Zhu, Side-chain cation-grafted poly(biphenyl piperidine) membranes for anion exchange membrane fuel cells, *J. Power Sources* 551 (2022) 232105–232116.
- [38] L. Yang, Z. Wang, F. Wang, Z. Wang, H. Zhu, Poly(aryl piperidinium) anion exchange membranes with cationic extender sidechain for fuel cells, *J. Membr. Sci.* 653 (2022) 120448–120459.
- [39] M.T. Guzmán-Gutiérrez, D.R. Nieto, S. Fomine, S.L. Morales, M.G. Zolotukhin, M.C. G. Hernandez, H. Kricheldorf, E.S. Wilks, Dramatic enhancement of superacid-catalyzed polyhydroxyalkylation reactions, *Macromolecules* 44 (2) (2011) 194–202.
- [40] T.H. Pham, J.S. Olsson, P. Jannasch, Effects of the N-alicyclic cation and backbone structures on the performance of poly(terphenyl)-based hydroxide exchange membranes, *J. Mater. Chem. A* 7 (26) (2019) 15895–15906.
- [41] Y. Zhu, Y. He, X. Ge, X. Liang, M.A. Shehzad, M. Hu, Y. Liu, L. Wu, T. Xu, A benzyltetramethylimidazolium-based membrane with exceptional alkaline stability in fuel cells: role of its structure in alkaline stability, *J. Mater. Chem. A* 6 (2018) 527–534.
- [42] W. Sheng, X. Zhou, L. Wu, Y. Shen, Y. Huang, L. Liu, S. Dai, N. Li, Quaternized poly(2,6-dimethyl-1,4-phenylene oxide) anion exchange membranes with pendant sterically-protected imidazoliums for alkaline fuel cells, *J. Membr. Sci.* 601 (2020) 117881–117890.
- [43] Y. Zheng, U. Ash, R.P. Pandey, A.G. Ozioko, J. Ponce-González, M. Handl, T. Weissbach, J.R. Varcoe, S. Holdcroft, M.W. Liberatore, R. Hiesgen, D.R. Dekel, Water uptake study of anion exchange membranes, *Macromolecules* 51 (9) (2018) 3264–3278.
- [44] D. Koronka, K. Miyatake, Anion exchange membranes containing no β-hydrogen atoms on ammonium groups: synthesis, properties, and alkaline stability, *RSC Adv.* 11 (2021) 1030–1038.
- [45] J.S. Olsson, T.H. Pham, P. Jannasch, Tuning poly(arylene piperidinium) anion-exchange membranes by copolymerization, partial quaternization and crosslinking, *J. Membr. Sci.* 578 (2019) 183–195.
- [46] T.H. Pham, J.S. Olsson, P. Jannasch, N-spirocyclic quaternary ammonium ionenes for anion-exchange membranes, *J. Am. Chem. Soc.* 139 (2017) 2888–2891.
- [47] X. Li, Q. Liu, Y. Yu, Y. Meng, Quaternized poly(arylene ether) ionomers containing triphenyl methane groups for alkaline anion exchange membranes, *J. Mater. Chem. A* 1 (2013) 4324–4335.
- [48] X. Chu, J. Liu, S. Miao, L. Liu, Y. Huang, E. Tang, S. Liu, X. Xing, N. Li, Crucial role of side-chain functionality in anion exchange membranes: Properties and alkaline fuel cell performance, *J. Membr. Sci.* 625 (2021) 119172–119183.
- [49] Z. Li, R. Yu, C. Liu, J. Zheng, J. Guo, T.A. Sherazi, S. Li, S. Zhang, Preparation and characterization of side-chain poly(aryl ether ketone) anion exchange membranes by superacid-catalyzed reaction, *Polymer* 222 (2021) 123639–123648.
- [50] N. Chen, C. Hu, H.H. Wang, J.H. Park, H.M. Kim, Y.M. Lee, Chemically & physically stable crosslinked poly(aryl-co-aryl piperidinium)s for anion exchange membrane fuel cells, *J. Membr. Sci.* 638 (2021) 119685–119695.
- [51] S. Chen, H. Peng, M. Hu, G. Wang, L. Xiao, J. Lu, L. Zhuang, Ultrathin self-cross-linked alkaline polymer electrolyte membrane for APEFC applications, *ACS Appl. Energy Mater.* 4 (5) (2021) 4297–4301.
- [52] X. Du, H. Zhang, Y. Yuan, Z. Wang, Constructing micro-phase separation structure to improve the performance of anion-exchange membrane based on poly(aryl piperidinium) cross-linked membranes, *J. Power Sour.* 487 (2021) 229429–229439.
- [53] T. Jiang, Y. Zhou, Y. Yang, C. Wu, H. Fang, S. Yang, H. Wei, Y. Ding, Dimensionally and oxidatively stable anion exchange membranes based on bication cross-linked poly(meta-terphenylene alkylene), *Polymer* 216 (2021) 123433–123442.
- [54] C. Long, Z. Wang, H. Zhu, High chemical stability anion exchange membrane based on poly(aryl piperidinium): Effect of monomer configuration on membrane properties, *Int. J. Hydrogen Energy* 46 (2021) 18524–18533.
- [55] X. Wang, R.G.H. Lammertink, Dimensionally stable multication-crosslinked poly(arylene piperidinium) membranes for water electrolysis, *J. Mater. Chem. A* 10 (15) (2022) 8401–8412.
- [56] L. Zhu, J. Pan, Y. Wang, J. Han, L. Zhuang, M.A. Hickner, Multication side chain anion exchange membranes, *Macromolecules* 49 (3) (2016) 815–824.

- [57] J. Han, L. Zhu, J. Pan, T.J. Zimudzi, Y. Wang, Y. Peng, M.A. Hickner, L. Zhuang, Elastic long-chain multication cross-linked anion exchange membranes, *Macromolecules* 50 (8) (2017) 3323–3332.
- [58] J. Han, J. Pan, C. Chen, L. Wei, Y.u. Wang, Q. Pan, N. Zhao, B.o. Xie, L.i. Xiao, J. Lu, L. Zhuang, Effect of micromorphology on alkaline polymer electrolyte stability, *ACS Appl. Mater. Interfaces* 11 (1) (2019) 469–477.
- [59] J. Han, Y. Zhang, F. Kang, C. Liu, W. Song, X. Zheng, X. Liu, M. Wang, X. Zhou, Z. Ren, M. Hu, L.i. Xiao, L. Zhuang, Poly(phenylene oxide)-based anion exchange membranes having linear cross-linkers or star cross-linkers, *ACS Appl. Energy Mater.* 5 (9) (2022) 11613–11623.
- [60] A. Barnett, J.J. Karnes, J. Lu, D.R. Major, J.S. Oakdale, K.N. Grew, J.P. McClure, V. Molinero, Exponential water uptake in ionomer membranes results from polymer plasticization, *Macromolecules* 55 (15) (2022) 6762–6774.
- [61] S. Willdorf-Cohen, A. Zhegur-Khais, J. Ponce-González, S. Bsoul-Haj, J.R. Varcoe, C.E. Diesendruck, D.R. Dekel, Alkaline stability of anion-exchange membranes, *ACS Appl. Energy Mater.* 6 (2) (2023) 1085–1092.
- [62] D.R. Dekel, M. Amar, S. Willdorf, M. Kosa, S. Dhara, C.E. Diesendruck, Effect of water on the stability of quaternary ammonium groups for anion exchange membrane fuel cell applications, *Chem. Mater.* 29 (10) (2017) 4425–4431.
- [63] S. Willdorf-Cohen, A. Kaushansky, D.R. Dekel, C.E. Diesendruck, Hydroxide chemoselectivity changes with water microsolvation, *J. Phys. Chem. Lett.* 13 (43) (2022) 10216–10221.
- [64] X. Gao, H. Yu, B. Qin, J. Jia, J. Hao, F. Xie, Z. Shao, Enhanced water transport in AEMs based on poly(styrene–ethylene–butylene–styrene) triblock copolymer for high fuel cell performance, *Polym. Chem.* 10 (15) (2019) 1894–1903.
- [65] K. Aggarwal, N. Gjineci, A. Kaushansky, S. Bsoul, J.C. Douglan, S. Li, I. Salam, S. Aharonovich, J.R. Varcoe, D.R. Dekel, C.E. Diesendruck, Isoindolinium groups as stable anion conductors for anion-exchange membrane fuel cells and electrolyzers, *ACS Mater. Au* 2 (3) (2022) 367–373.
- [66] Z.H. Cai, X.L. Gao, W.T. Gao, Y.S.L. Choo, J.J. Wang, Q.G. Zhang, A.M. Zhu, Q. Liu, Effect of hydrophobic side chain length on poly(carbazolyl terphenyl piperidinium) anion exchange membranes, *ACS Appl. Energy Mater.* 5 (8) (2022) 10165–10176.
- [67] M.S. Cha, J.E. Park, S. Kim, S.-H. Han, S.-H. Shin, S.H. Yang, T.-H. Kim, D.M. Yu, S. So, Y.T. Hong, S.J. Yoon, S.-G. Oh, S.Y. Kang, O.-H. Kim, H.S. Park, B. Bae, Y.-E. Sung, Y.-H. Cho, J.Y. Lee, Poly(carbazole)-based anion-conducting materials with high performance and durability for energy conversion devices, *Energy Environ. Sci.* 13 (10) (2020) 3633–3645.
- [68] L. Ma, M. Hussain, L. Li, N.A. Qaisrani, L. Bai, Y. Jia, X. Yan, F. Zhang, G. He, Octopus-like side chain grafted poly(arylene piperidinium) membranes for fuel cell application, *J. Membr. Sci.* 636 (2021) 119529–119539.
- [69] X. Hu, Y. Huang, L. Liu, Q. Ju, X. Zhou, X. Qiao, Z. Zheng, N. Li, Piperidinium functionalized aryl ether-free polyaromatics as anion exchange membrane for water electrolyzers: Performance and durability, *J. Membr. Sci.* 621 (2021) 118964–118976.
- [70] L. Liu, L. Bai, Z. Liu, S. Miao, J. Pan, L. Shen, Y. Shi, N. Li, Side-chain structural engineering on poly(terphenyl piperidinium) anion exchange membrane for water electrolyzers, *J. Membr. Sci.* 665 (2023) 121135–121145.
- [71] P. Fortin, T. Khoza, X. Cao, S.Y. Martinsen, A. Oyarce Barnett, S. Holdcroft, High-performance alkaline water electrolysis using Aemion™ anion exchange membranes, *J. Power Sources* 451 (2020) 227814–227824.
- [72] N. Chen, S.Y. Paek, J.Y. Lee, J.H. Park, S.Y. Lee, Y.M. Lee, High-performance anion exchange membrane water electrolyzers with a current density of 7.68 A cm^{-2} and a durability of 1000 hours, *Energy Environ. Sci.* 14 (12) (2021) 6338–6348.
- [73] R. Soni, S. Miyanishi, H. Kuroki, T. Yamaguchi, Pure water solid alkaline water electrolyzer using fully aromatic and high-molecular-weight poly(fluorene-alt-tetrafluorophenylene)-trimethyl ammonium anion exchange membranes and ionomers, *ACS Appl. Energy Mater.* 4 (2) (2021) 1053–1058.
- [74] M.S. Cha, J.E. Park, S. Kim, S.-H. Shin, S.H. Yang, S.J. Lee, T.-H. Kim, D.M. Yu, S. So, K.M. Oh, Y.-E. Sung, Y.-H. Cho, J.Y. Lee, Oligomeric chain extender-derived anion conducting membrane materials with poly(p-phenylene)-based architecture for fuel cells and water electrolyzers, *J. Mater. Chem. A* 10 (17) (2022) 9693–9706.
- [75] H. Lim, I. Jeong, J. Choi, G. Shin, J. Kim, T.H. Kim, T. Park, Anion exchange membranes and ionomer properties of a polyfluorene-based polymer with alkyl spacers for water electrolysis, *Appl. Surf. Sci.* 610 (2023) 155601–155606.